



## Fragment-based design of 3-aminopyridine-derived amides as potent inhibitors of human nicotinamide phosphoribosyltransferase (NAMPT)



Peter S. Dragovich<sup>a,\*</sup>, Guiling Zhao<sup>a</sup>, Timm Baumeister<sup>b</sup>, Brandon Bravo<sup>a</sup>, Anthony M. Giannetti<sup>a</sup>, Yen-Ching Ho<sup>b</sup>, Rongbao Hua<sup>c</sup>, Guangkun Li<sup>c</sup>, Xiaorong Liang<sup>a</sup>, Xiaolei Ma<sup>a</sup>, Thomas O'Brien<sup>a</sup>, Angela Oh<sup>a</sup>, Nicholas J. Skelton<sup>a</sup>, Chengcheng Wang<sup>d</sup>, Weiru Wang<sup>a</sup>, Yunli Wang<sup>c</sup>, Yang Xiao<sup>a</sup>, Po-wai Yuen<sup>c</sup>, Mark Zak<sup>a</sup>, Qiang Zhao<sup>d</sup>, Xiaozhang Zheng<sup>b</sup>

<sup>a</sup> Genentech, Inc., 1 DNA Way, South San Francisco, CA 94080, USA

<sup>b</sup> Forma Therapeutics, Inc., 500 Arsenal Street, Watertown, MA 02472, USA

<sup>c</sup> Pharmaron Beijing, Co. Ltd., 6 Taihe Road, BDA, Beijing 100176, PR China

<sup>d</sup> Crown Bioscience, Science & Technology Innovation Park, No.6 Beijing West Road, Taicang City, Jiangsu Province, PR China

### ARTICLE INFO

#### Article history:

Received 17 October 2013

Revised 12 December 2013

Accepted 16 December 2013

Available online 21 December 2013

#### Keywords:

Nicotinamide phosphoribosyltransferase  
NAMPT

Fragment-based design

Structure-based design

X-ray crystal structure

Surface plasmon resonance

### ABSTRACT

The fragment-based identification of two novel and potent biochemical inhibitors of the nicotinamide phosphoribosyltransferase (NAMPT) enzyme is described. These compounds (**51** and **63**) incorporate an amide moiety derived from 3-aminopyridine, and are thus structurally distinct from other known anti-NAMPT agents. Each exhibits potent inhibition of NAMPT biochemical activity ( $IC_{50}$  = 19 and 15 nM, respectively) as well as robust antiproliferative properties in A2780 cell culture experiments ( $IC_{50}$  = 121 and 99 nM, respectively). However, additional biological studies indicate that only inhibitor **51** exerts its A2780 cell culture effects via a NAMPT-mediated mechanism. The crystal structures of both **51** and **63** in complex with NAMPT are also independently described.

© 2013 Elsevier Ltd. All rights reserved.

Nicotinamide phosphoribosyltransferase (NAMPT, also known in the literature as pre-B cell colony-enhancing factor (PBEF) as well as visfatin; EC 2.4.2.12) plays a critical role in cellular metabolism.<sup>1</sup> The enzyme catalyzes the rate-limiting step in the conversion of nicotinamide (NAM) to the important enzyme co-factor nicotinamide adenine dinucleotide (NAD).<sup>2</sup> This process enables the efficient intracellular recycling of NAM, which is produced by the catalytic action of NAD-consuming enzymes such as the PARPs and Sirtuins, back into NAD (Fig. 1).<sup>3</sup> Proper maintenance of NAD levels is known to be critical to sustaining energetics required for many cellular functions.<sup>4</sup> Inhibition of NAMPT has therefore emerged as a novel strategy for impairing the proliferation of tumors whose high growth rates may make them more susceptible to NAMPT disruption relative to non-cancerous cells.<sup>5</sup>

Multiple examples of NAMPT inhibitors are known in the scientific and patent literature, and the most advanced of these agents [GMX-1778 (**1**)<sup>6</sup> and APO-866 (**2**)<sup>7</sup>; Fig. 2] have progressed to hu-

man clinical trials.<sup>8,9</sup> Our own prior discovery efforts identified potent urea and amide-derived NAMPT inhibitors which also contained terminal biaryl sulfone moieties (compounds **3–6**; Fig. 2).<sup>10</sup> In an effort to further diversify these molecules, we also conducted a surface plasmon resonance (SPR)-based screen to identify small, structurally novel NAMPT-binding moieties ('fragments') which could be combined with our existing compounds.<sup>11</sup> In this report, we describe the structure-based elaboration of two SPR screening hits into potent anti-NAMPT agents that are structurally distinct from other known NAMPT inhibitors.

Compound **7** was identified from our SPR-based screening methods as a moderately potent NAMPT binder with high ligand efficiency (Table 1).<sup>11,12</sup> The compound also demonstrated the ability to inhibit NAMPT in biochemical assessments, although its potency was somewhat attenuated relative to its binding properties (Table 1).<sup>13</sup> A co-crystal structure of the molecule in complex with NAMPT was subsequently determined and revealed that the molecule occupied the nicotinamide-binding region of the protein's active site (Fig. 3).<sup>14</sup> Not unexpectedly, the pyridine portion of **7** formed face-to-face pi-stacking interactions with the side

\* Corresponding author.

E-mail address: [dragovich.peter@gene.com](mailto:dragovich.peter@gene.com) (P.S. Dragovich).

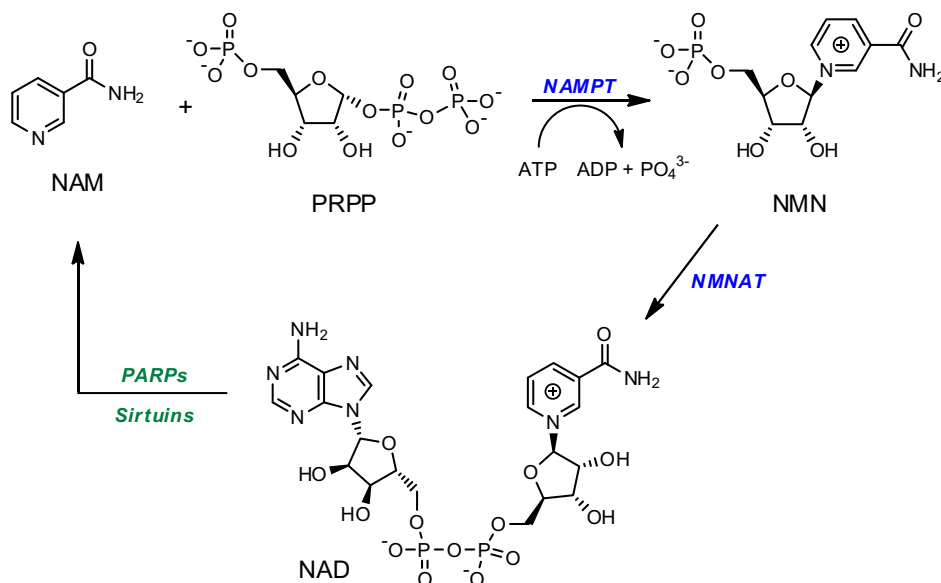


Figure 1. NAD recycling and NAMPT biochemical mechanism.

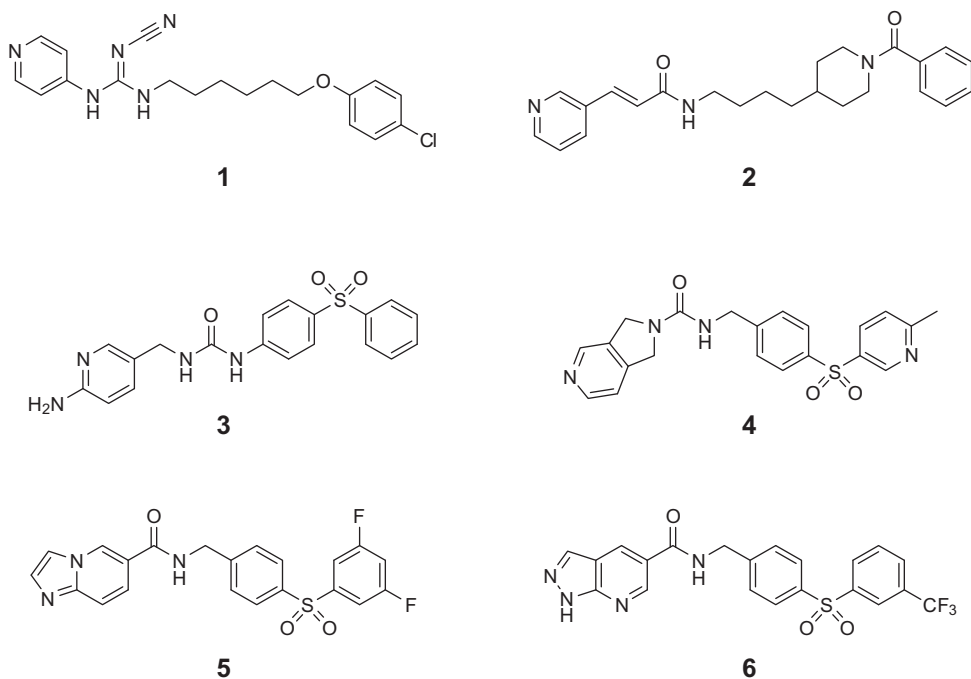


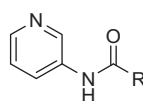
Figure 2. Examples of known NAMPT inhibitors.

chains of Phe-193 and Tyr-18' in a manner that was similar to that observed for many other NAMPT inhibitors.<sup>10</sup> A hydrogen bond was also observed between the amide NH of **7** and the NAMPT Asp-219 residue. However, in contrast to the binding of previously-studied amide-containing NAMPT inhibitors such as **5**,<sup>10c</sup> the amide moiety of **7** was positioned much deeper in the nicotinamide-binding region of the protein (Fig. 3). This location oriented the amide carbonyl of **7** directly toward the Arg-311 side chain instead of toward a water-filled region of the active site that was typically occupied by the carbonyl group present in other known NAMPT inhibitors (e.g., **4–6**, Fig. 2).<sup>10c–e</sup> Importantly, the observed binding of **7** positioned the compound's pyridine nitrogen in a location that was similar to that observed for the N-atoms present in many other heterocycles which bound to the same NAMPT

region (e.g., compare the location of the imidazopyridine moiety present in **5** with that of the pyridine contained in **7**; Fig. 3). Such positioning was consistent with **7** functioning as a NAMPT substrate and undergoing enzyme-catalyzed condensation with PRPP in the NAMPT active site, although this possibility was not examined experimentally (c.f., Fig. 1).<sup>15</sup>

Our first attempts to improve the inhibitory activity of **7** involved replacing the N-methyl-pyrazole moiety with other isosteric methyl-containing heterocycles. However, as shown in Table 1, none of these modifications afforded significant improvements in SPR-binding affinity to NAMPT or biochemical inhibitory activity (compare **7** with compounds **8–16**).<sup>16</sup> Attempts to extend various methyl-containing heterocycles into the NAMPT tunnel region occupied by the benzyl portion of **5** (c.f., Fig. 3) were also not

**Table 1**  
Initial SAR of 3-aminopyridine-amide NAMPT inhibitors



Compd	R	NAMPT IC <sub>50</sub> <sup>a</sup> (uM)	NAMPT K <sub>d</sub> <sup>b</sup> (uM)	NAMPT SPR LE <sup>c</sup>
7		91	5.2	0.47
8		>100	176	0.36
9		>100	129	0.35
10		34	36	0.40
11		>100	55	0.38
12		38	12	0.44
13		>100	61	0.38
14		50	129	0.35
15		>100	20	0.42
16		>100	13	0.44

All biochemical and SPR results are reported as the arithmetic mean of at least 2 separate runs.

<sup>a</sup> NAMPT biochemical inhibition.

<sup>b</sup> NAMPT SPR binding.

<sup>c</sup> Ligand efficiency based on SPR K<sub>d</sub> value.

successful. This outcome was obtained regardless of whether the extending moieties were appended to a position adjacent to (compounds **17–20**) or once-removed from (compounds **21–23**) the heterocyclic methyl group (Table 2). These results collectively indicated that replacement of the methyl-pyrazole present in **7** with non-isosteric and/or structurally diverse moieties would likely be required to properly optimize the potency of the 3-aminopyridine-amide inhibitor series.

Accordingly, crystal structures of several other NAMPT fragment screening hits were determined to identify those with good potential for combination with lead compound **7**.<sup>11</sup> The nitro-substituted benzimidazole **24** (Fig. 4), which exhibited moderate SPR-based NAMPT affinity and good ligand efficiency, emerged from this exploration as a particularly attractive possibility. As shown in Fig. 5, the compound bound to NAMPT in the tunnel region with the nitro group located near where the amide moiety of **7** resided in the **7**-NAMPT crystal structure. A hydrogen bond was observed between one nitro group oxygen atom of **24** and the side chain of Arg-311 which was shifted from its location in the **7**-NAMPT crystal structure in order to facilitate this interaction. The benzimidazole portion of **24** formed many favorable van der

Waals contacts with hydrophobic portions of the NAMPT tunnel region (Ile-309, Ile-351, and the face of His-191) but did not interact with any observed water molecules. Somewhat unexpectedly, the benzimidazole of **24** did not bind to NAMPT in a manner that was co-planar with the methyl-pyrazole contained in **7**. However, analysis of the two overlaid structures suggested that replacement of the latter moiety with a simple phenyl ring would be tolerated and would offer alternate vectors for further elaboration into the NAMPT tunnel region (Fig. 5).

As shown in Table 3, effecting the described substitution afforded a molecule (**25**) with significantly improved biochemical NAMPT inhibitory activity relative to lead compound **7**. Importantly, extension of **25** via modification of the 4-position on the phenyl ring was typically tolerated and often improved biochemical potency as compared to the unsubstituted inhibitor (**26–35**; Table 3). Two notable exceptions to this trend were the amino-containing molecules **29** and **32** which, based on the **24**-NAMPT co-crystal structure, unfavorably positioned their polar amino groups in the center of the hydrophobic NAMPT tunnel region. Encouragingly, however, transformation of the amine moieties present in either compound to the corresponding carbamates

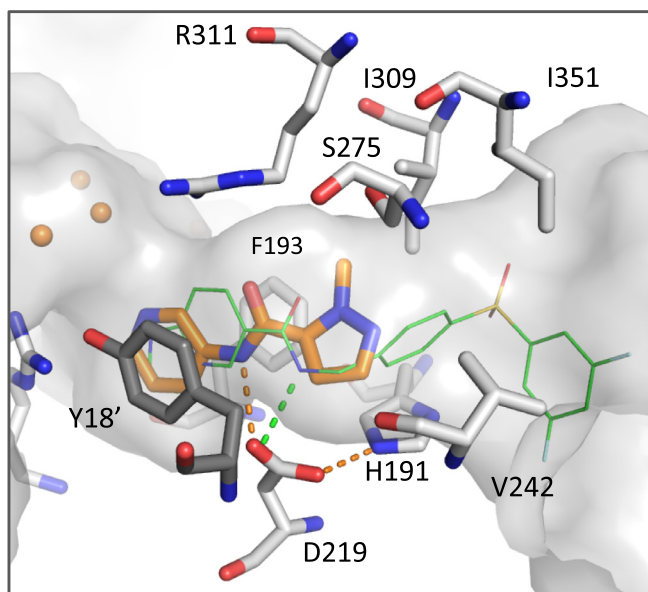


**Figure 3.** Crystal structure of compound **7** in complex with NAMPT (resolution = 2.86 Å; PDB accession code 4N9B). Protein side chains from the two NAMPT monomers which form the dimeric active site cleft are depicted in white and grey, respectively. The van der Waals surface of the ligand binding pocket is also shown in grey. The inhibitor is presented as orange tubes with corresponding crystallographic water molecules and hydrogen bonds indicated by orange spheres and dashed orange lines, respectively. The thin green lines depict the location of compound **5** in the binding site (PDB accession code 4KFO). Hydrogen bond interactions between **5** and NAMPT are indicated by the dashed green lines.

and/or sulfonamides afforded molecules with more promising NAMPT inhibition properties (**30–31** and **33–35**). This observation prompted us to systematically explore appending phenyl-containing acyl and sulfonyl moieties to the amines present in **29** and **32**. We anticipated that some of the resulting compounds would successfully traverse the NAMPT tunnel region and interact with a post-tunnel (solvent-exposed) area of the protein in a manner similar to that noted for the terminal portions of larger known NAMPT inhibitors (e.g., compound **1–6**, Fig. 2; see also Figs. 3 and 6–8).

Table 4 depicts the outcome of this systematic exploration. Molecules incorporating benzoyl-derived amides were moderately potent NAMPT inhibitors when the amides were directly attached to the compounds' central phenyl rings (**36**, **40**, **44**, and **48**). However, inclusion of a methylene moiety between the amides and the central phenyl rings significantly impaired the potencies of the resulting compounds (**37**, **41**, **45**, and **49**). In contrast, direct central-ring attachment of phenyl-containing sulfonamides afforded ineffective NAMPT inhibitors (**38**, **42**, **46**, and **50**) while extension of the same sulfonamide moieties by a methylene group provided much more potent inhibitors (**39**, **43**, **47**, **51**). The ability of several compounds contained in Table 4 to inhibit the proliferation of A2780 cells was also tested. Most molecules did not exhibit meaningful activity in this assessment, likely due to insufficient NAMPT inhibition potency. However, compounds **47** and **51** displayed measurable anti-proliferation activity and the latter (more potent) molecule was selected for additional characterization studies.

The co-crystal structure of inhibitor **51** in complex with NAMPT is shown in Figure 6. The molecule's amino-pyridine fragment bound to the protein in a manner that was very similar to, although not quite co-planar with, the binding mode described above for the identical portion of compound **7**. Accordingly, the pyridine ring of **51** was situated between the side chains of Phe-193 and Tyr-18' and a hydrogen bond was observed between the compound's amide NH moiety and the Asp-219 residue. The central phenyl ring of inhibitor **51** occupied the NAMPT tunnel region and was

**Table 2**  
Elaboration of 3-aminopyridine-amide NAMPT inhibitors

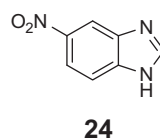
Compd	R	NAMPT IC <sub>50</sub> <sup>a</sup> (μM)	NAMPT K <sub>d</sub> <sup>b</sup> (μM)	NAMPT SPR LE <sup>c</sup>
<b>17</b>		>100	234	0.31
<b>18</b>		>100	>500	NA
<b>19</b>		>100	177	0.24
<b>20</b>		>100	>500	NA
<b>21</b>		>100	59	0.36
<b>22</b>		>100	233	0.29
<b>23</b>		>100	481	0.26

All biochemical and SPR results are reported as the arithmetic mean of at least 2 separate runs.

<sup>a</sup> NAMPT biochemical inhibition.

<sup>b</sup> NAMPT SPR binding.

<sup>c</sup> Ligand efficiency based on SPR K<sub>d</sub> value (NA = not applicable).



NAMPT SPR K<sub>D</sub> = 126 μM  
NAMPT SPR LE = 0.44

**24**

**Figure 4.** NAMPT fragment screening hit.

positioned similarly to both the methyl-pyrazole present in **7** and the benzimidazole contained in **24**. However, the phenyl group of **51** was not precisely co-planar with either of these entities and instead filled a space in the tunnel region that resided between them. This orientation was drastically different from the binding mode observed previously for the central benzyl group of compound **5** in the same area of the protein (Fig. 6). In contrast, the terminal phenyl-sulfonamide portion of **51** interacted with NAMPT in a manner that was very similar to that noted for the terminal sulfone present in **5** with water-mediated hydrogen bonds being formed with both sulfonamide oxygen atoms (Fig. 6). The pyridine N-atom of **51** was situated very close to the exposed imidazopyridine nitrogen of **5** in the NAMPT nicotinamide binding region, and this positioning was consistent with **51** possibly functioning as a NAMPT substrate.<sup>15</sup> The collective analysis of the **51**-NAMPT co-crystal structure demonstrated how a compound that was structurally distinct from other known NAMPT inhibitors such as compounds **3–6** could effectively and uniquely occupy the protein's active site.<sup>17</sup>

Further analysis of the **24**-NAMPT co crystal structure described above (Fig. 5) suggested that 6,5-bicyclic aromatic moieties could

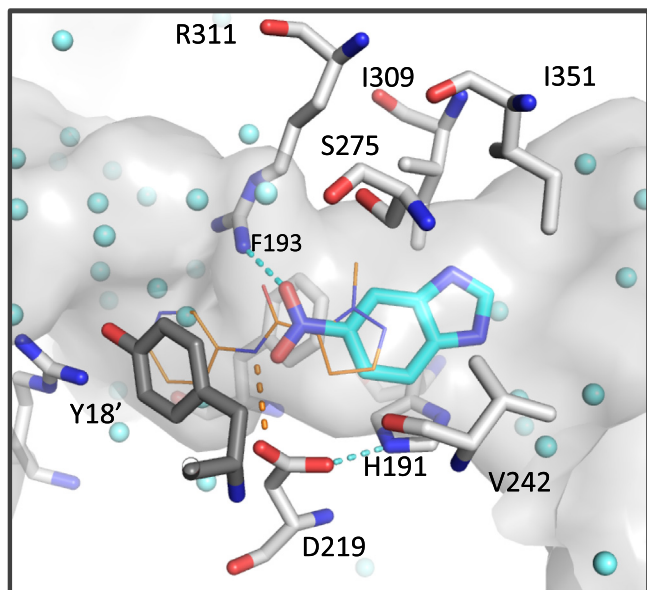
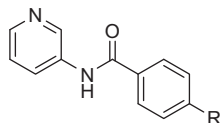


**Figure 5.** Crystal structure of compound **24** in complex with NAMPT (resolution = 1.75 Å; PDB accession code 4N9C). Protein side chains from the two NAMPT monomers which form the dimeric active site cleft are depicted in white and grey, respectively. The van der Waals surface of the ligand binding pocket is also shown in grey. The inhibitor is presented as cyan tubes with corresponding crystallographic water molecules and hydrogen bonds indicated by cyan spheres and cyan lines, respectively. The thin orange lines depict the location of compound **7** in the binding site (PDB accession code 4N9B). Hydrogen bond interactions between **7** and NAMPT are indicated by the dashed orange lines.

**Table 3**  
Additional elaboration of 3-aminopyridine-amide NAMPT inhibitors



Compd	R	NAMPT IC <sub>50</sub> <sup>a</sup> (μM)
<b>25</b>	H	13
<b>26</b>	CH <sub>3</sub>	13
<b>27</b>	Ph	1.0
<b>28</b>	Cyclohexyl	1.0
<b>29</b>	NH <sub>2</sub>	>100
<b>30</b>	NHBoc	0.42
<b>31</b>	NHSO <sub>2</sub> CH <sub>3</sub>	10.3
<b>32</b>	CH <sub>2</sub> NH <sub>2</sub>	>100
<b>33</b>	CH <sub>2</sub> NHBoc	13
<b>34</b>	CH <sub>2</sub> NHCbz	3.3
<b>35</b>	CH <sub>2</sub> NHSO <sub>2</sub> CH <sub>3</sub>	5.0

All biochemical results are reported as the arithmetic mean of at least 2 separate runs.

<sup>a</sup> NAMPT biochemical inhibition.

also be productively utilized as replacements for the methylpyrazole present in fragment lead **7**. Accordingly, a benzimidazole containing an appropriately-positioned 3-amino-pyridine-derived amide displayed encouraging biochemical NAMPT inhibitory activity (compound **52**, Table 5). Replacement of the benzimidazole present in **52** with several other 6,5-bicyclic aromatic systems also afforded biochemically active NAMPT inhibitors (**53–58**, Table 5), although several compound potencies were somewhat attenuated relative to that exhibited by **52**. Unfortunately, all of these molecules failed to demonstrate anti-NAMPT activity in cell culture assessments. These outcomes were not entirely surprising since the compound concentrations tested in these cell-based

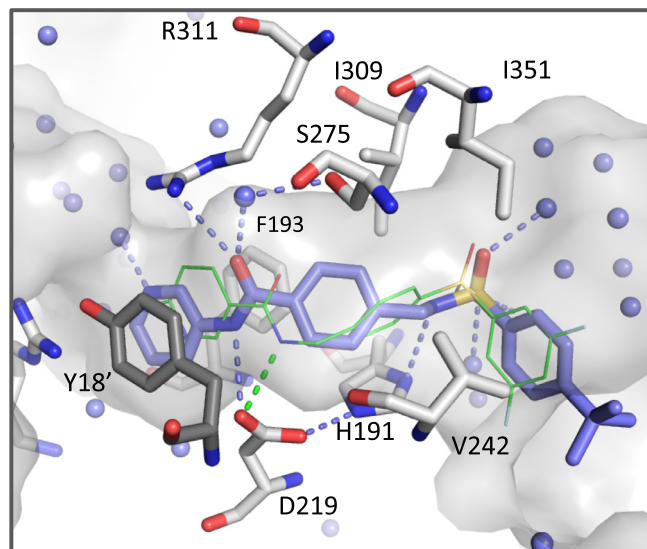


**Figure 6.** Crystal structure of compound **51** in complex with NAMPT (resolution = 1.70 Å; PDB accession code 4N9D). Protein side chains from the two NAMPT monomers which form the dimeric active site cleft are depicted in white and grey, respectively. The van der Waals surface of the ligand binding pocket is also shown in grey. The inhibitor is presented as blue tubes with corresponding crystallographic water molecules and hydrogen bonds indicated by blue spheres and dashed blue lines, respectively. The thin green lines depict the location of compound **5** in the binding site (PDB accession code 4KFO). Hydrogen bond interactions between **5** and NAMPT are indicated by the dashed green lines.

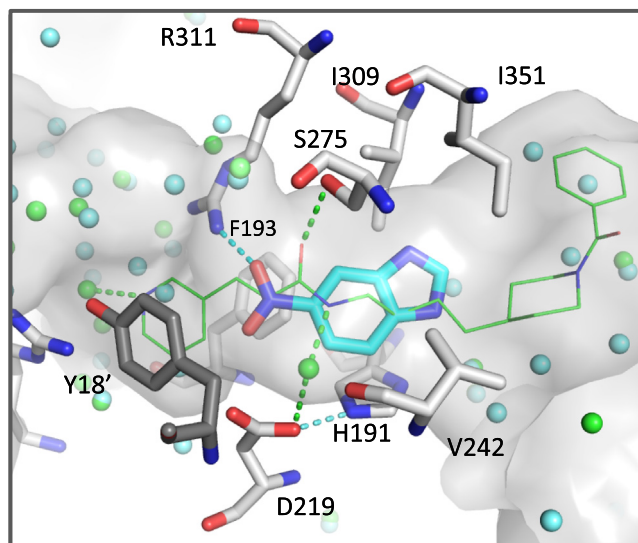


**Figure 7.** Crystal structure of compound **24** in complex with NAMPT (resolution = 1.75 Å; PDB accession code 4N9C). Protein side chains from the two NAMPT monomers which form the dimeric active site cleft are depicted in white and grey, respectively. The van der Waals surface of the ligand binding pocket is also shown in grey. The inhibitor is presented as cyan tubes with corresponding crystallographic water molecules and hydrogen bonds indicated by cyan spheres and dashed cyan lines, respectively. The thin green lines depict the location of compound **2** in the binding site (PDB accession code 2GVJ). Hydrogen bond interactions between **2** and NAMPT are indicated by the dashed green lines.

experiments were somewhat low relative to the corresponding biochemical IC<sub>50</sub> values. Attempts to further elaborate the benzimidazole contained in **52** by derivatizing the nitrogen atom *meta* to the carboxamide substituent were unsuccessful (compounds **59** and **60**, Table 5). However, analysis of the bound conformations of fragment **24** and the very potent NAMPT inhibitor **2** suggested that



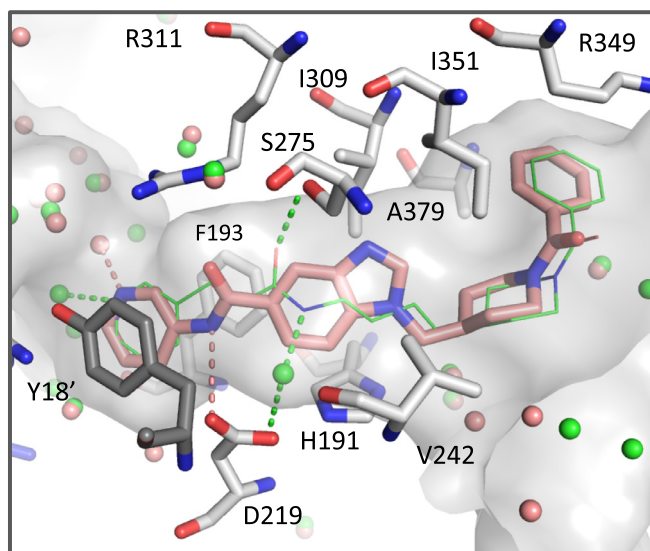


**Figure 8.** Crystal structure of compound **63** in complex with NAMPT (resolution = 1.72 Å; PDB accession code 4N9E). Protein side chains from the two NAMPT monomers which form the dimeric active site cleft are depicted in white and grey, respectively. The van der Waals surface of the ligand binding pocket is also shown in grey. The inhibitor is presented as salmon tubes with corresponding crystallographic water molecules and hydrogen bonds indicated by salmon spheres and dashed salmon lines, respectively. The thin green lines depict the location of compound **2** in the binding site (PDB accession code 2GVJ). Hydrogen bond interactions between **2** and NAMPT are indicated by the dashed green lines.

**Table 4**

Systematic exploration of amino-containing 3-aminopyridine-amide NAMPT inhibitors

Compd	R	X	n	NAMPT IC <sub>50</sub> <sup>a</sup> (μM)	A2780 IC <sub>50</sub> <sup>b</sup> (μM)
<b>36</b>		C=O	0	0.61	>2.0
<b>37</b>		C=O	1	25	ND
<b>38</b>		SO <sub>2</sub>	0	>100	>2.0
<b>39</b>		SO <sub>2</sub>	1	0.21	ND
<b>40</b>		C=O	0	1.5	>2.0
<b>41</b>		C=O	1	40	ND
<b>42</b>		SO <sub>2</sub>	0	83	>2.0
<b>43</b>		SO <sub>2</sub>	1	0.014	ND
<b>44</b>		C=O	0	0.64	>2.0
<b>45</b>		C=O	1	3.1	>2.0
<b>46</b>		SO <sub>2</sub>	0	62	>2.0
<b>47</b>		SO <sub>2</sub>	1	0.019	0.88
<b>48</b>		C=O	0	0.29	>2.0
<b>49</b>		C=O	1	80	ND
<b>50</b>		SO <sub>2</sub>	0	36	>2.0
<b>51</b>		SO <sub>2</sub>	1	0.019	0.12

All biochemical and cell-based results are reported as the arithmetic mean of at least 2 separate runs.

<sup>a</sup> NAMPT biochemical inhibition.

<sup>b</sup> Antiproliferation activity determined in cell culture experiments using A2780 cell line (ND = not determined). This inhibition can be reversed by addition of 0.33 mM of NMN.

functionalization of the **52** nitrogen atom *para* to the carboxamide substituent might be more fruitful (Fig. 7). Specifically, it was envisioned that introduction of a methyl group at this location in **52** would be tolerated and would thereby enable additional

**Table 5**

3-Aminopyridine-amide NAMPT inhibitors containing 6,5-bicyclic moieties

Compd	R	NAMPT IC <sub>50</sub> <sup>a</sup> (μM)	A2780 IC <sub>50</sub> <sup>b</sup> (μM)
<b>52</b>		1.5	>2.0
<b>53</b>		9.1	>2.0
<b>54</b>		3.4	>2.0
<b>55</b>		26	>2.0
<b>56</b>		4.1	>2.0
<b>57</b>		21	>2.0
<b>58</b>		21	ND
<b>59</b>		>100	ND
<b>60</b>		>100	ND

All biochemical and cell-based results are reported as the arithmetic mean of at least 2 separate runs.

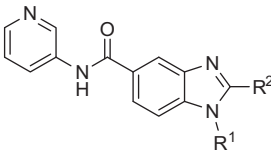
<sup>a</sup> NAMPT biochemical inhibition.

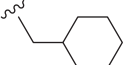
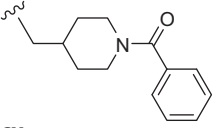
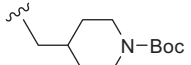
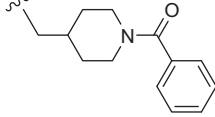
<sup>b</sup> Antiproliferation activity determined in cell culture experiments using A2780 cell line. ND = not determined.

elaboration with molecular fragments derived directly from the structure of inhibitor **2**.

The described methyl-containing derivative of **52** was prepared (compound **61**) and it displayed biochemical NAMPT inhibition properties that were equivalent to those exhibited by the unmethylated parent molecule (Table 6). Further elaboration of the methyl group present in **61** with several moieties inspired by the structure of inhibitor **2** was either tolerated (**62**) or dramatically improved biochemical NAMPT inhibitory activity (**63**). However, related derivatization of the **61** benzimidazole 2-position weakened anti-NAMPT potency with the larger appended groups having the most deleterious effects (compounds **64–67**, Table 6). Cell-culture antiproliferation effects were assessed with several of the compounds depicted in Table 6, but only inhibitor **63** exhibited significant potency in these experiments. Somewhat surprisingly, however, the antiproliferative effects associated with **63** were not completely reversed/eliminated by the addition of NMN (the biochemical product of NAMPT catalysis; c.f. Fig. 1) to the cell culture media. This result suggested that the cell effects

**Table 6**  
Optimization of benzimidazole-containing 3-aminopyridine-amide NAMPT inhibitors



Compd	R <sup>1</sup>	R <sup>2</sup>	NAMPT IC <sub>50</sub> <sup>a</sup> (μM)	A2780 IC <sub>50</sub> <sup>b</sup> (μM)
<b>52</b>	H	H	1.5	>2.0
<b>61</b>	CH <sub>3</sub>	H	1.4	ND
<b>62</b>		H	3.7	>2.0
<b>63</b>		H	0.015	0.099 <sup>c</sup>
<b>64</b>	CH <sub>3</sub>	CH <sub>3</sub>	6.1	ND
<b>65</b>	CH <sub>3</sub>	Ph	14	ND
<b>66</b>	CH <sub>3</sub>		>100	ND
<b>67</b>	CH <sub>3</sub>		>100	ND

All biochemical and cell-based results are reported as the arithmetic mean of at least 2 separate runs.

<sup>a</sup> NAMPT biochemical inhibition.

<sup>b</sup> Antiproliferation activity determined in cell culture experiments using A2780 cell line (ND = not determined).

<sup>c</sup> Antiproliferative effects were only partially reversed by addition of 0.33 mM of NMN.

**Table 7**  
Antiproliferation effects determined for compounds **51** and **63** in various human tumor cell lines<sup>a,b</sup>

	CyQuant IC <sub>50</sub> values in nM			
	HT1080	PC3	MiaPaCa2 <sup>c</sup>	HCT116
<b>51</b>	213 ± 9	217 ± 67	855 ± 77	271 ± 31
<b>63</b>	>1000	>1000	>1000	>1000

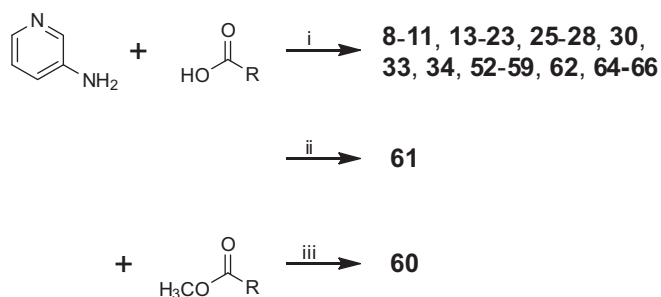
<sup>a</sup> CyQuant endpoint; arithmetic mean of 3 separate runs (*n* = 3, standard deviations are also shown).

<sup>b</sup> All antiproliferation effects were reversed by addition of 330 μM NMN, strongly implicating NAMPT inhibition as the causative MOA.

<sup>c</sup> *n* = 2. See [Supplementary data](#) for experimental details.

observed for compound **63** might result from inhibition of biological targets in addition to and/or other than NAMPT. More detailed characterization studies of compound **63** were therefore undertaken to better explore this possibility.

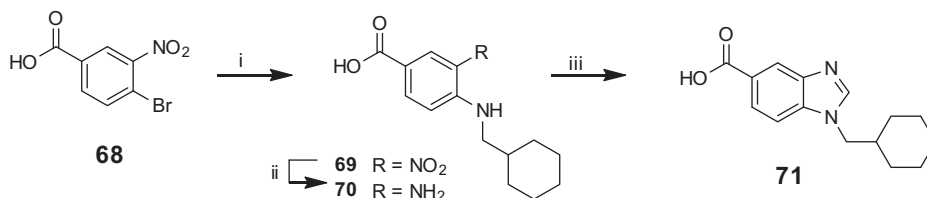
A co-crystal structure of compound **63** in complex with NAMPT was determined and it confirmed that the compound could biophysically associate with the protein. The terminal portion of the molecule, which bound in the post-tunnel, solvent-exposed NAMPT region, closely mimicked the bound conformation of the corresponding portion of inhibitor **2** (Fig. 8). Such binding enabled many favorable van der Waals contacts between the benzoyl moiety present in **63** and aliphatic portions of the side chains of NAMPT residues Arg-349 and Ala-379. Similar favorable van der Waals interactions were also noted between the piperidine fragment of **63** and the hydrophobic Val-242 and Ile-309 NAMPT tunnel-region residues. As was observed for other 3-amino-pyridine amides described in this work, the pyridine portion of **63** formed face-to-face pi-stacking interactions with the side chains of Phe-193 and Tyr-18', a hydrogen bond existed between the compound's amide NH and Asp-219, and the molecule's amide carbonyl was



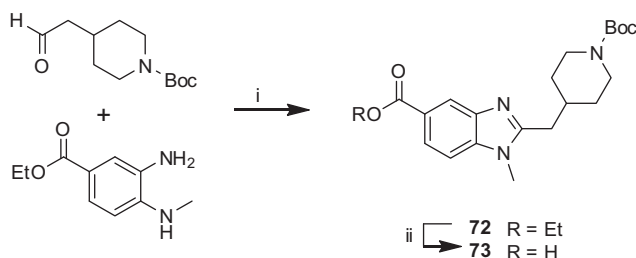
**Scheme 1.** Synthesis of compounds containing 3-aminopyridine-derived amides. Reagents and conditions: (i) HATU, (*i*-Pr)<sub>2</sub>NEt, DMF, 25–50 °C, 3–18 h, 4–76%; (ii) HATU, (*i*-Pr)<sub>2</sub>NEt, DMF, 45 °C, 3 h (forms HOAt adduct), then 3-aminopyridine, microwave, DMF, 95 °C, 1 h, 25%; (iii) AlCl<sub>3</sub>, 1,2-dichloroethane, 70 °C, 15 h, 35%.

oriented directly toward the Arg-311 side chain. As also expected from analysis of many inhibitor–NAMPT co-crystal structures, the pyridine nitrogen atoms of compounds **63** and **2** were located in similar positions in the NAM-binding region of the protein that were consistent with each molecule possibly functioning as a NAMPT substrate.<sup>15</sup>

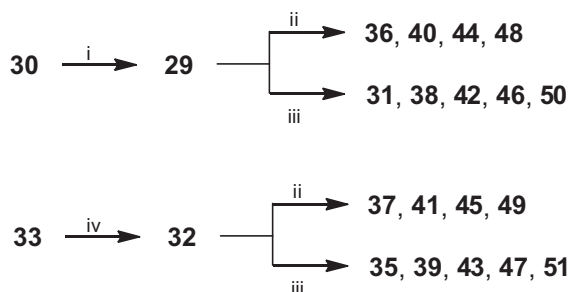
In addition to the various studies described above, more extensive cell-culture experiments were conducted with both compounds **51** and **63** to characterize their anti-NAMPT properties in greater detail. Compound **51** potently reduced NAD levels in A2780 cells with an IC<sub>50</sub> value between 24 and 58 nM (Figs. S1 and S2). In contrast, compound **63** exhibited negligible effects on A2780 NAD levels when tested under similar experimental conditions (IC<sub>50</sub> >1000 nM; Fig. S3). The latter observation was consistent with the inability of NMN to reverse the A2780 antiproliferation effects exhibited by compound **63** and suggested that, in spite of the compound's ability to biophysically associate



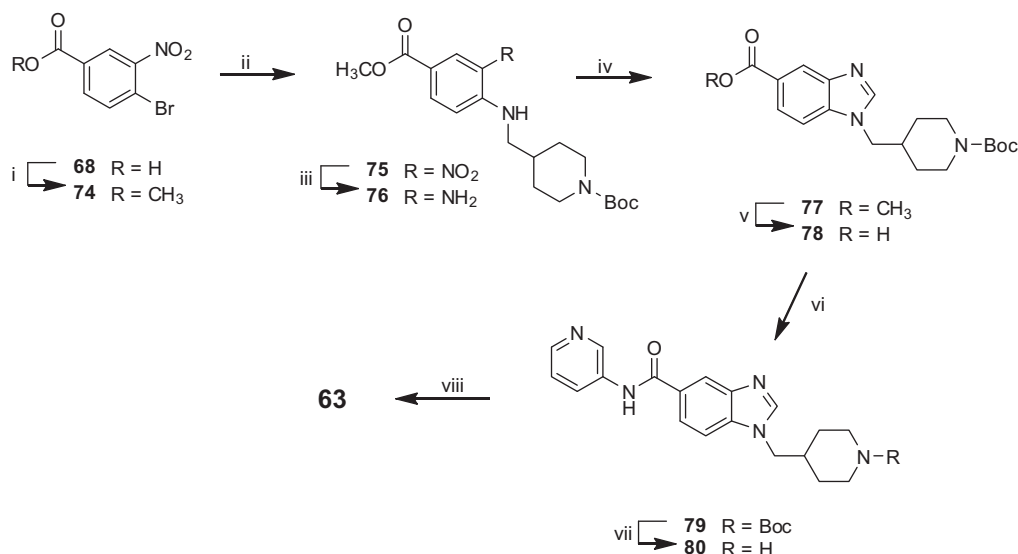
**Scheme 2.** Synthesis of acid required to prepare compound **62**. Reagents and conditions: (i) Cyclohexylmethanamine,  $K_2CO_3$ , DMF, 110 °C, 14 h, 19%; (ii)  $H_2$ , 10% Pd on C, MeOH, 25 °C, 2 h, 91%; (iii)  $HC(OEt)_3$ , EtOH, 70 °C, 14 h, 87%.



**Scheme 3.** Synthesis of acid required to prepare compound **66**. Reagents and conditions: (i) 10% Pd/C, EtOH, reflux, 48 h, 89%; (ii) 1:5 1 N NaOH:EtOH, 85 °C, 18 h, 94%.



**Scheme 4.** Alternate synthesis of amide and sulfonamide-containing compounds. Reagents and conditions: (i) 4.0 M HCl, 1,4-dioxane, 25 °C, 6 h, 85%; (ii)  $RC(O)Cl$ ,  $Et_3N$ ,  $CH_2Cl_2$ , 25 °C, 18 h, 11–26%; (iii)  $RSO_2Cl$ ,  $(i-Pr)_2NEt$ ,  $CH_2Cl_2$ , 25 °C, 18 h, 4–45%; (iv) TFA,  $CH_2Cl_2$ , 25 °C, 3 h, 90%.



**Scheme 5.** Synthesis of compound **63**. Reagents and conditions: (i) EDC-HCl,  $(i-Pr)_2NEt$ , HOBT, MeOH, 25 °C, 1 h, 87%; (ii) *tert*-butyl-4-(aminomethyl)piperidine-1-carboxylate,  $K_2CO_3$ , DMF, 100 °C, 20 h, 65%; (iii) Raney Ni,  $H_2$ , MeOH, 25 °C, 0.5 h, 45%; (iv) PPTS,  $HC(OEt)_3$ ,  $CH_2Cl_2$ , 25 °C, 20 h, 72%; (v) KOH, EtOH/ $H_2O$ , 25 °C, 20 h, 82%; (vi) 3-aminopyridine, HATU,  $(i-Pr)_2NEt$ , DMF, 25 °C, 20 h, 55%; (vii) TFA,  $CH_2Cl_2$ , 25 °C, 0.5 h, 82%; (viii)  $PhC(O)Cl$ ,  $Et_3N$ ,  $CH_2Cl_2$ , 25 °C, 0.5 h, 14%.

with the protein and potentially inhibit its biochemical activity, the A2780 cell culture outcomes likely result from non-NAMPT-related biological activity. Accordingly, compound **63** did not exhibit meaningful antiproliferative effects against four other cancer cell lines against which it was tested (Table 7). Encouragingly, however, compound **51**, which strongly reduced NAD levels in A2780 cells, exhibited potent to moderate antiproliferative activity against all of these same lines (Table 7). Taken together, the above results indicate that careful biological characterization should be conducted with novel NAMPT inhibitors to confirm that any observed antiproliferative effects truly result from inhibition of the targeted NAMPT enzyme.

The compounds described in this work were either purchased from Sigma–Aldrich (**7**, **12**, and **24**) or were prepared by the methods shown in Schemes 1–5.<sup>18</sup> Many were synthesized by HATU-mediated coupling of commercially available carboxylic acids with 3-aminopyridine (**8**–**11**, **13**–**23**, **25**–**28**, **30**, **33**, **34**, **52**–**58**, **62**, **64**–**66**; Scheme 1). The acid required for the preparation of compound **59** was obtained by hydrolysis of the corresponding (commercially available) methyl ester while those needed to make **62** and **66** were prepared as described in Schemes 2 and 3, respectively. In the case of inhibitor **60**, the desired amide linkage was formed directly from 3-aminopyridine and the appropriate methyl ester using an  $AlCl_3$ -mediated coupling technique (Scheme 1). Removal of the Boc groups present in compounds **30** and **33** using various acidic conditions respectively afforded the amino-containing molecules **29** and **32** in good yield. These entities were subsequently transformed into the corresponding amides and sulfonamides by reaction with various acid- and sulfonyl-chlorides (compounds **31**, **35**–**51**; Scheme 4). The preparation of compound **63** was



somewhat more complicated and was accomplished by the synthesis depicted in [Scheme 5](#).

In this report, we describe the fragment-based identification of two potent biochemical inhibitors of the nicotinamide phosphoribosyltransferase enzyme that are structurally distinct from other known anti-NAMPT agents. Each of these new compounds (**51** and **63**) incorporates an amide moiety derived from 3-aminopyridine, and this entity enables them to bind to NAMPT in a manner that is unique relative to how other NAMPT inhibitors associate with the protein. Although both compounds exhibit antiproliferative activity in A2780 cell culture experiments, only inhibitor **51** appears to exert these effects via a NAMPT-mediated mechanism. This molecule also displays antiproliferative properties in several other cancer cell lines. Collectively, our results provide new chemical options for the design of potent NAMPT inhibitors, and also caution regarding the need for careful biological characterization of any novel molecules so identified.

## Acknowledgments

We thank Drs. Krista Bowman and Jiansheng Wu and their respective Genentech research groups for performing many protein expression and purification activities. We also thank Shohini Ganguly for generating all the biochemical and cell IC<sub>50</sub> results. Finally, we thank Dr. Peter Jackson for many helpful discussions regarding NAMPT and Dr. Jeff Blaney for many useful suggestions associated with fragment-based ligand design.

## Supplementary data

Supplementary data associated with this article can be found, in the online version, at <http://dx.doi.org/10.1016/j.bmcl.2013.12.062>.

## References and notes

- (a) He, J.; Tu, C.; Li, M.; Wang, S.; Guan, X.; Lin, J.; Li, Z. *Curr. Pharm. Des.* **2012**, *18*, 6123; (b) Burgos, E. S. *Curr. Med. Chem.* **2011**, *18*, 1947; (c) Bi, T.-Q.; Che, M. *Cancer Biol. Ther.* **2010**, *10*, 119; (d) Garten, A.; Petzold, S.; Körner, A.; Imai, S.-I.; Kiess, W. *Trends Endocrin. Metab.* **2008**, *20*, 130.
- (a) Houtkooper, R. H.; Cantó, C.; Wanders, R. J.; Auwerx, J. *Endocrine Rev.* **2010**, *31*, 194; (b) Sauve, A. A. *J. Pharmacol. Exp. Ther.* **2008**, *324*, 883.
- The de novo NAD synthesis pathway requires eight enzyme-catalyzed steps to produce the co-factor from tryptophan. See Ref. 2 for additional details.
- (a) Schulze, A.; Harris, A. L. *Nature* **2012**, *491*, 364; (b) Ward, P. S.; Thompson, C. B. *Cancer Cell* **2012**, *21*, 297; (c) Jones, N. P.; Schulze, A. *Drug Discovery Today* **2012**, *17*, 232; (d) Tennant, D. A.; Durán, R. V.; Gottlieb, E. *Nat. Rev. Cancer* **2010**, *10*, 267; (e) Vander Heiden, M. G.; Cantley, L. C.; Thompson, C. B. *Science* **2009**, *324*, 1029.
- (a) Chiarugi, A.; Dölle, C.; Felici, R.; Ziegler, M. *Nat. Rev. Cancer* **2012**, *12*, 741; (b) Zhang, L. Q.; Heruth, D. P.; Ye, S. Q. *J. Bioanal. Biomed.* **2011**, *3*, 13; (c) Khan, J. A.; Forouhar, F.; Tao, X.; Tong, L. *Exp. Opin. Ther. Targets* **2007**, *11*, 695.
- (a) Watson, M.; Roulston, A.; Bélec, L.; Billot, X.; Marcellus, R.; Bédard, D.; Bernier, C.; Branchaud, S.; Chan, H.; Dai, K.; Gilbert, K.; Goulet, D.; Gratton, M.-O.; Isakau, H.; Jang, A.; Khadir, A.; Koch, E.; Lavoie, M.; Lawless, M.; Nguyen, M.; Paquette, D.; Turcotte, E.; Berger, A.; Mitchell, M.; Shore, G. C.; Beauparlant, P. *Mol. Cell. Biol.* **2009**, *29*, 5872; (b) Ravaut, A.; Cerny, T.; Terret, C.; Wanders, J.; Bui, B. N.; Hess, D.; Droz, J.-P.; Fumoleau, P.; Twelves, C. *Eur. J. Cancer* **2005**, *41*, 702; (c) Hovstad, P.; Larsson, R.; Jonsson, E.; Skov, T.; Kissmeyer, A.-M.; Krasilnikoff, K.; Bergh, J.; Karlsson, M. O.; Lonnebo, A.; Ahlgren, J. *Clin. Cancer Res.* **2002**, *8*, 2843. Compound 1 is also known in the literature as CHS828.
- (a) Holen, K.; Saltz, L. B.; Hollywood, E.; Burk, K.; Hanauske, A.-R. *Invest. New Drugs* **2008**, *26*, 45; (b) Hasmann, M.; Schemainda, I. *Cancer Res.* **2003**, *63*, 7436. Compound 2 is also known in the literature as FK866.
- For a recent review of NAMPT and associated inhibitors, see Galli, U.; Travelli, C.; Massarotti, A.; Fakhouri, G.; Rahimian, R.; Tron, G. C.; Genazzani, A. A. *J. Med. Chem.* **2013**, *56*, 6279.
- (a) Christensen, M. K.; Erichsen, K. D.; Olesen, U. H.; Tjørnelund, J.; Fristrup, P.; Thougard, A.; Nielsen, S. J.; Sehested, M.; Jensen, P. B.; Loza, E.; Kalvinsh, I.; Garten, A.; Kiess, W.; Björklund, F. *J. Med. Chem.* **2013**, *56*, 9071; (b) Arigon, J.; Bernhart, C.; Bouaboula, M.; Dimalta, A.; Nardi, F.; Jegham, S. WO 2012038904, **2012**; (c) Arigon, J.; Bernhart, C.; Bosch, M.; Bouaboula, M.; Nardi, F.; Jegham, S.; Combet, R. WO 2012038905, **2012**; (d) Curtin, M. L.; Sorensen, B. K.; Heyman, H. R.; Clark, R. F.; Woller, K. R.; Michaelides, M.; Tse, C.; Vasudevan, A.; Mack, H.; Hansen, T. M.; Sweis, R.; Plushchev, M. A. US 2012022842, **2012**; (e) Curtin, M. L.; Sorensen, B. K.; Heyman, H. R.; Clark, R. F.; Michaelides, M.; Tse, C. US 2012022924, **2012**; (f) Kumar, D. V.; Slattum, P. M.; Yager, K. M.; Shenderovich, M. D.; Tangallapally, R.; Kim, S. WO 2012177782, **2012**; (g) Willardsen, A. J.; Lockman, J. W.; Murphy, B. R.; Judd, W. R.; Kim, I. C.; Kim, S.-H.; Zigar, D. F.; Yager, K. M.; Fleischer, T. C.; Terry-Lorenzo, R. T.; Boniface, J. J.; Parker, D. P.; McAlexander, I. A.; Bursavich, M. G.; Dastrup, D. M. WO 201109441, **2011**; (h) You, H.; Youn, H.-S.; Im, I.; Bae, M.-H.; Lee, S.-K.; Ko, H.; Eom, S. H.; Kim, Y.-C. *Eur. J. Med. Chem.* **2011**, *46*, 1153; (i) Lockman, J. W.; Murphy, B. R.; Zigar, D. F.; Judd, W. R.; Slattum, P. M.; Gao, Z.-H.; Ostanin, K.; Green, J.; McKinnon, R.; Terry-Lorenzo, R. T.; Fleischer, T. C.; Boniface, J. J.; Shenderovich, M.; Willardsen, J. A. *J. Med. Chem.* **2010**, *53*, 8734; (j) Colombano, G.; Travelli, C.; Galli, U.; Caldarelli, A.; Chini, M. G.; Canonico, P. L.; Sorba, G.; Bifulco, G.; Tron, G. C.; Genazzani, A. A. *J. Med. Chem.* **2010**, *53*, 616; (k) Galli, U.; Ercolano, E.; Carraro, L.; Blasi Roman, C. R.; Sorba, G.; Canonico, P. L.; Genazzani, A. A.; Tron, G. C.; Billington, R. A. *ChemMedChem* **2008**, *3*, 771.
- (a) Zheng, X.; Bauer, P.; Baumeister, T.; Buckmelter, A. J.; Caligiuri, M.; Clodfelter, K. H.; Han, B.; Ho, Y.-C.; Kley, N.; Lin, J.; Reynolds, D. J.; Sharma, G.; Smith, C. C.; Wang, Z.; Dragovich, P. S.; Oh, A.; Wang, W.; Zak, M.; Gunzner-Toste, J.; Zhao, G.; Yuen, P.-W.; Bair, K. W. *J. Med. Chem.* **2013**, *56*, 4921; (b) Gunzner-Toste, J.; Zhao, G.; Bauer, P.; Baumeister, T.; Buckmelter, A. J.; Caligiuri, M.; Clodfelter, K. H.; Fu, B.; Han, B.; Ho, Y.-C.; Kley, N.; Liang, X.; Liederer, B. M.; Lin, J.; Mukadam, S.; O'Brien, T.; Oh, A.; Reynolds, D. J.; Sharma, G.; Skelton, N.; Smith, C. C.; Sodhi, J.; Wang, W.; Wang, Z.; Xiao, Y.; Yuen, P.-W.; Zak, M.; Zhang, L.; Zheng, X.; Bair, K. W.; Dragovich, P. S. *Bioorg. Med. Chem. Lett.* **2013**, *23*, 3531; (c) Zheng, X.; Bauer, P.; Baumeister, T.; Buckmelter, A. J.; Caligiuri, M.; Clodfelter, K. H.; Han, B.; Ho, Y.-C.; Kley, N.; Lin, J.; Reynolds, D. J.; Sharma, G.; Smith, C. C.; Wang, Z.; Dragovich, P. S.; Gunzner-Toste, J.; Liederer, B. M.; Ly, J.; O'Brien, T.; Oh, A.; Wang, L.; Wang, W.; Xiao, Y.; Zak, M.; Zhao, G.; Yuen, P.-W.; Bair, K. W. *J. Med. Chem.* **2013**, *56*, 6413; (d) Dragovich, P. S.; Bair, K. W.; Baumeister, T.; Ho, Y.-C.; Liederer, B. M.; Liu, X.; Liu, Y.; O'Brien, T.; Oeh, J.; Sampath, D.; Skelton, N.; Wang, L.; Wang, W.; Wu, H.; Xiao, Y.; Yuen, P.-W.; Zak, M.; Zhang, L.; Zheng, X. *Bioorg. Med. Chem. Lett.* **2013**, *23*, 4875; (e) Zheng, X.; Bair, K. W.; Bauer, P.; Baumeister, T.; Bowman, K. K.; Buckmelter, A. J.; Caligiuri, M.; Clodfelter, K. H.; Feng, Y.; Han, B.; Ho, Y.-C.; Kley, N.; Li, H.; Liang, X.; Liederer, B. M.; Lin, J.; Ly, J.; O'Brien, T.; Oeh, J.; Oh, A.; Reynolds, D. J.; Sampath, D.; Sharma, G.; Skelton, N.; Smith, C. C.; Tremayne, J.; Wang, L.; Wang, W.; Wang, Z.; Wu, H.; Xiao, Y.; Yang, G.; Yuen, P.-W.; Zak, M.; Dragovich, P. S. *Bioorg. Med. Chem. Lett.* **2013**, *23*, 5488.
- Giannetti, A. M.; Zheng, X.; Skelton, N. J.; Wang, W.; Bravo, B.; Bair, K. W.; Baumeister, T.; Cheng, E.; Crocker, L.; Feng, Y.; Gunzner-Toste, J.; Ho, Y.-C.; Hua, R.; Liederer, B. M.; Liu, Y.; Ma, X.; O'Brien, T.; Oeh, J.; Sampath, D.; Shen, Y.; Wang, C.; Wang, L.; Wu, H.; Xiao, Y.; Yuen, P.-W.; Zak, M.; Zhao, G.; Zhao, Q.; Dragovich, P. S. submitted to *J. Med. Chem.*
- Hopkins, A. L.; Groom, C. R.; Alex, A. *Drug Discovery Today* **2004**, *9*, 430.
- The SPR assessments omitted the PRPP co-substrate and ATP additive that were included in the biochemical inhibition assays (c.f., [Fig. 1](#)). The latter entity is known in the literature to improve NAMPT catalytic efficiency (see: Burgos, E. S.; Schramm, V. L. *Biochemistry* **2008**, *47*, 11086). Thus, it was not surprising that that SPR K<sub>d</sub> values did not perfectly correspond to biochemical IC<sub>50</sub> measurements. SPR techniques were utilized primarily to identify the novel NAMPT binding fragments and to optimize their affinity in the absence of meaningful biochemical inhibitory activity. Once biochemical IC<sub>50</sub> values of <20 μM were achieved for a given inhibitor series, biochemical methods were preferentially used in subsequent optimization activities.
- NAMPT is believed to function as a symmetrical homodimer with two active sites formed at opposite ends of the dimer interface. Accordingly, the protein crystallized with such a dimer present in the asymmetric unit. The two monomer chains in the dimers of the co-crystal structures described in this work were very similar, and both active sites contained co-crystallized molecules in similar orientations. In the crystallography discussions, the NAMPT residues are designated with prime and non-prime notation (e.g., Tyr18', Phe193) to distinguish the monomer chain in which a given residue resides.
- We currently believe that many cell-potent NAMPT inhibitors form PRPP-derived phosphoribosylated adducts in the protein's active site which block the function of the enzyme. This belief is consistent with the repeated observation of these adducts by mass spectrometry in biochemical and/or crystallographic experiments (e.g., compounds **5** and **6**; see Ref. 10a,c,e). Once formed, the PRPP-adducts may accumulate intracellularly and thereby enhance cell culture antiproliferation effects (see Ref. 6a for additional information and discussion). However, there are many other factors that also likely influence NAMPT inhibitor cell potency including: biochemical inhibition activity, the ability of a given inhibitor and/or its corresponding PRPP-derived ribose adduct to effectively compete with the NAM substrate, cell membrane permeability, and/or protein binding.
- The improvements in biochemical inhibition exhibited by compounds **10**, **12**, and **14** relative to **7** were deemed too incremental to warrant additional follow-up activities.
- Compound **51** was previously described in the literature as STF-31, an inhibitor of the GLUT1 glucose transporter: Chan, D. A.; Sutphin, P. D.; Nguyen, P.; Turcotte, S.; Lai, E. W.; Banh, A.; Reynolds, G. E.; Chi, J.-T.; Wu, J.; Solow-Cordero, D. E.; Bonnet, M.; Flanagan, J. U.; Bouley, D. M.; Graves, E. E.; Denny, W. A.; Hay, M. P.; Giaccia, A. J. *Sci. Trans. Med.* **2011**, *3*, 94ra70.
- The chemical purities of all final compounds described in this work were >95% as determined by as determined by LCMS analysis with UV detection at 220 nm.